Hull-Appendage Interaction of a Sailing Yacht, Investigated with Wave-Cut Techniques

Jonathan R. Binns, Australian Maritime Engineering Cooperative Research Centre (AMECRC)
Kim Klaka, Australian Maritime Engineering Cooperative Research Centre (AMECRC)
Andrew Dovell, Iain Murray & Associates Pty Ltd

ABSTRACT

The research explained in this paper was carried out to investigate the effects of hull-appendage interaction on the resistance of a sailing yacht, and the effects these changes have on the velocity prediction for a sailing yacht. To accomplish this aim a series of wave-cut experiments was carried out and analysed using a modified procedure. The processed results have then been incorporated into an existing velocity prediction program. For the purposes of this research two variables were investigated for the Australian Maritime Engineering Cooperative Research Centre (AMECRC) parent model 004, a model derived from the Delft IMS series of yachts.

Wave-cut procedures inevitably raise questions about scaling procedures for full scale extrapolation as the inviscid wave-pattern resistance is calculated to be less than the residuary or wave resistance. These questions have been dealt with by an approximate method, briefly explained in this paper.

NOTATION

A	Wetted surface area of model (m^2)
ARe	Effective aspect ratio of lifting surface
ARg	Geometric aspect ratio
Cdi	Induced drag coefficient
Cf	Skin friction resistance coefficient
Cl	Lift coefficient
Ct	Total resistance coefficient
Cw	Assumed wave resistance or residuary resistance coefficient
Cwp	Wave-pattern resistance coefficient
Di	Induced drag due to three-dimensional lift production (N)
Fn	Froude number
GPR	General Purpose Rating (seconds per nautical mile)
IMS	International Measurement System
k	Form factor
k_Δ	Form factor calculated from wave-pattern results, can vary with yacht speed
L	Lift (N)
LR	Linear Random
Rf	Skin friction resistance (N)
Rn	Reynolds number
Rt	Total resistance (N)
Rv	Total viscous resistance (N)
Rw	Assumed wave resistance or residuary resistance (N)
Rwp	Wave-pattern resistance (N)
s	Span of lifting surface (m)
S	Profile area of lifting surface (m^2)
Vs	Yacht full scale predicted velocity (knots)
VPP	Velocity Prediction Program
x	Longitudinal dimension, aft positive
y	Transverse dimension, starboard positive
z	Vertical dimension, against gravity positive
ρ	Fluid density (kg/m^3)
ψ	Yaw angle of yacht (degrees)
ζ	Wave height (m)

INTRODUCTION

The primary objective of the research has been to provide design information as to the effect of sailing yacht hull and appendage characteristics on the resistance of the yacht. It has been observed in yacht model tests that varying the appendages on a sailing hull appears to have the effect of changing the wave-pattern around the yacht (for example see Rosen et al, 1993). Therefore the wave-pattern was analysed by conducting a wave-cut program.

The variables investigated were the keel rudder separation and the rudder angle. To investigate the overall effects of the appendages the model was also

tested with no appendages, with keel only and with rudder only. Fig. 1 shows the six profiles of the models that were tested. It was found that the best performance prediction was obtained by locating the rudder as far aft as possible, with the smallest rudder angle possible. However, the steps taken in this research required some assumptions, which should guide the applications of this basic design principle (see Binns, 1996).

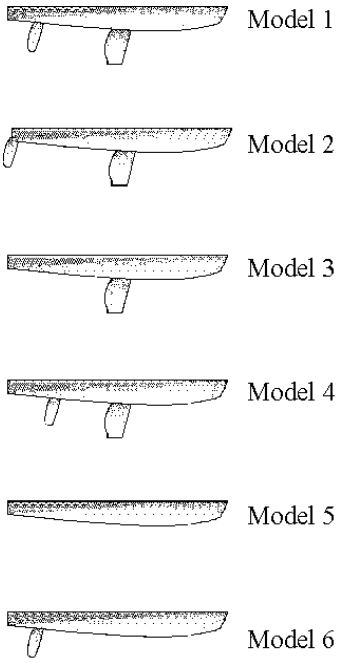

Fig. 2 Model configurations tested

By using wave-cut techniques it is possible to shed some light on the subject of scaling the results from the model to the prototype yachts. It has been concluded from this research that using a standard resistance scaling scheme the wave-pattern resistance is probably being overestimated, resulting in a 12% over prediction of the total resistance.

The tank tests required for this research were carried out in the AMECRC towing tank based at the Australian Maritime College (AMC), Launceston, Tasmania. The tank has a rectangular cross section with a length of 60 m, width of 3.5 m and depth of 1.5 m.

DIVISION OF RESISTANCE

Basic Principles

In order to analyse the resistance of a sailing yacht it is extremely useful to divide the total resistance into components. This is because the total resistance is due to fairly distinct phenomena and so different assumptions may be made for each component allowing for different prediction methods to be employed. Furthermore, the division of resistance becomes critical when work is to be carried out at model scale and extrapolated to full scale.

The resistance of a sailing yacht may be divided into three broad groups. The first group is that associated with gravity forces, the second that concerned with viscous forces and the third that due to the generation of lift on a three-dimensional body. The first group can be described by the wave surface energy around the yacht. The second and third groups can be observed and evaluated by measurements of the detailed sub-surface velocity field around the hull. Then these three components of resistance may be added to give the total resistance, easily measured at model scale as the force required to tow the vessel.

A hierarchy of yacht resistance could be visualised as follows

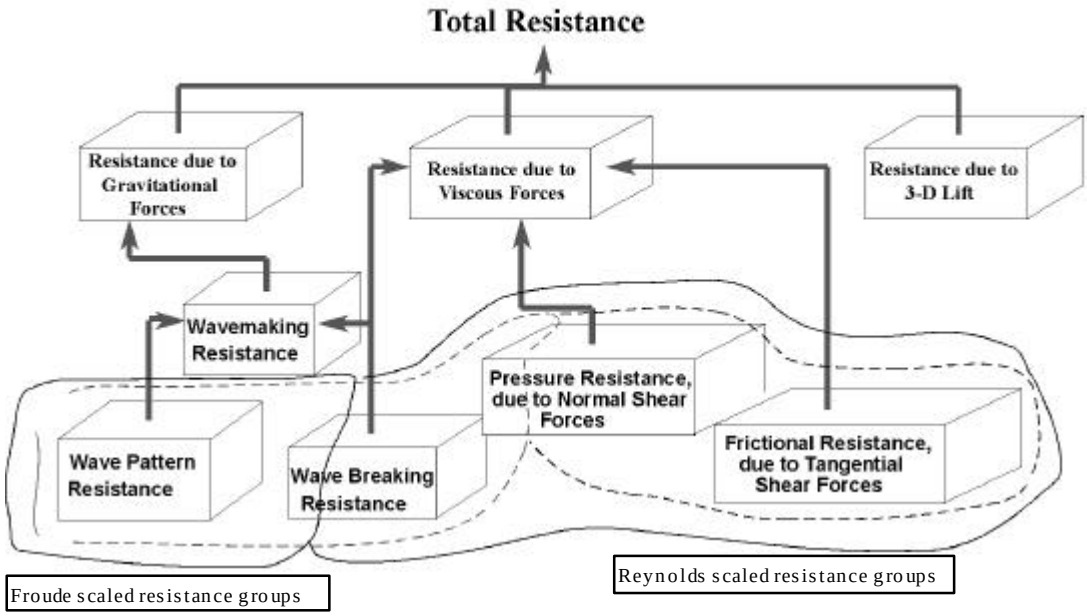

Fig. 3 Resistance hierarchy diagram.

In this diagram wave-breaking resistance is seen to contribute to two resistance components. Also on the diagram groupings of resistance components have been shown for Reynolds and Froude scaling portions. The dashed lines show where traditional scaling methods divide the total resistance, and the solid lines show where wave-cut guided scaling methods divide the resistance. This shall be discussed in the following sections.

Mainly due to the thin nature of most ships, the resistance due to viscous effects can be fairly well predicted by approximating the vessel to a flat plate. The third resistance group can be accurately predicted by potential flow theory at small angles of attack. By using these assumptions the wave resistance can be measured by subtracting the calculated viscous resistance from the total resistance. Generally this procedure is sufficient when separation of the flow around the vessel is small.

In order to create side forces sailing yachts usually need to advance through the water with an angle of yaw. The side force can then be created by a symmetric lifting surface, for example a keel. The angle of yaw also creates a lot more separation around the hull and so increases the viscous resistance. This increase cannot be described by the use of a simple skin friction coefficient. Therefore in order to separate the resistance due to waves and the viscous resistance it is necessary to measure one or the other. If the relationship between wave height and wave energy is known, the wave-pattern resistance can be determined by measuring the wave-pattern around the yacht (Eggers et al, 1967); this is the basis of the research described here.

Scaling of Resistance Components

The laws of similitude have been well documented in the past and so will not be dealt with here (see for example Harvald, 1983, pp 39-42), suffice to say that viscous resistance requires Reynolds scaling whereas resistance due to gravitational forces requires Froude scaling.

A traditional approach to the problem of scaling model resistance which seems to be fairly widely used is that first described by Hughes and later modified by Prohaska (see Hughes, 1966). This method involves using a skin friction coefficient such as

$$Cf = \frac{0.075}{\left(\log_{10} Rn - 2\right)^2}, \qquad (1)$$

where Rn is the Reynolds number. The total viscous resistance will be a multiple of this skin friction coefficient, to account for the viscous resistance difference between a flat plate equivalent and the model. This multiple, or form factor, can be calculated by extrapolating the total resistance to a zero Froude number equivalent, at which point the resistance will be entirely viscous. Then it is required to assume that the form factor will not change with

Froude number, thus allowing it to be used at any model or full scale speed.

The viscous resistance can then be subtracted from the total resistance of the model to give the residuary resistance, which is assumed to be the wave resistance. This procedure can be illustrated by the following equation

$$Rw = Rt - (1+k)Rf\,, \qquad (2)$$

where Rw is the assumed wave resistance, Rt is the total resistance, k is the form factor and Rf is the frictional resistance. All of these values are for model scale. At this point the total resistance of the vessel has been sufficiently decomposed for it to be extrapolated up to full scale. This can be done by scaling the wave resistance by Froude scaling and then predicting the viscous resistance for the appropriate full scale Reynolds number. The skin friction formula quoted above can be used with the form factor calculated from model results to give the full scale total viscous resistance.

A modification to this basic procedure is one of the final outputs of the research described here. By performing a wave-cut on a model yacht it is possible to determine how much energy (therefore resistance) is required to produce the wave-pattern around the vessel. This energy could therefore be thought of as the true wave-pattern resistance for the yacht, which is the portion of the resistance which requires Froude scaling.

A POSSIBLE SCALING PROCEDURE USING WAVE-CUT RESULTS

Upright Resistance Analysis

By using wave-cut analysis the actual inviscid resistance associated with the generation of waves can be calculated, the coefficient of this resistance is called Cwp. By subtracting this coefficient from the total an effective zero Froude number condition can be obtained. Then defining the form factor as an expression of the difference between the resistance of a flat plate and that of the specific vessel at zero Froude number, the form factor could be calculated using the following formula

$$(1+k_{\Delta})Cf = Ct - Cwp\,. \qquad (3)$$

When k_{Δ} is calculated it is found to vary with model speed. Then it is required to assume that the value of k_{Δ} will remain constant for a model and a full scale prototype at the same Froude number, yaw, heel, rudder angle and keel rudder separation and is independent of Reynolds number. The total viscous resistance can then be thought of as being partly Froude scaled and partly Reynolds scaled as the Cf value is Reynolds number dependent.

Yawed Resistance Analysis

The decomposition of the yawed resistance for the models presents an extra variable to that of the upright case. When a three-dimensional foil produces lift it leaves trailing vortices and a starting vortex. The energy for these vortices has to come from the foil and is seen by the foil as an addition to the drag. For the purposes of this research this extra drag will be termed induced drag. It must be noted, however, that this induced drag is not the total addition to the drag due to yaw. The total drag due to yaw would consist of additions to all components of resistance. The induced drag thus defined does not include lift-induced wave-pattern resistance measured using wave-cut data, because the induced drag is due to vortices generated away from the wave survey area. It was considered undesirable to put the induced drag into the form factor k_{Δ} as the comparison to upright runs could lead to incorrect conclusions. Therefore an estimate for the induced drag was required.

Basic Theory

By consideration of the downwash induced by the trailing vortices, the induced drag can be calculated for irrotational ideal flow, see Duncan et al, 1970, pp 604-607. The result is that the induced drag coefficient can be calculated from

$$Cdi = \frac{Cl^2}{\pi\ ARe}\,, \qquad (4)$$

where ARe is the effective aspect ratio for an elliptic lift distribution. The effects of not having an elliptic lift distribution can be assumed to be included in the calculation of the ARe. Also in Equation (5) Cl is the lift coefficient defined by

$$Cl = \frac{L}{0.5\rho Vs^2 S}\,, \qquad (6)$$

where L is the total lift from the foil, ρ is the water density, Vs is the flow velocity and S is the profile area of the foil. Similarly, Cdi is defined as

$$Cdi = \frac{Di}{0.5\rho Vs^2 S}\,, \qquad (7)$$

where Di is the induced drag. The effective aspect ratio, ARe, must be calculated from experimental results, and then Cdi can be converted to be non-dimensionalised with respect to the wetted surface area of the model, so that it can be compared to other drag coefficients.

Calculation of ARe

Assuming that all other components of the resistance remain constant with Cl, then from Equation (8) ARe can be calculated from the slope of

the graph of Ct to Cl^2. From the wave-cut analysis it is immediately apparent that the Cwp coefficient rises steadily with yaw angle for high speeds, therefore in order to calculate Cdi directly from the slope, it is required to assume that the change in k_Δ exactly offsets the growth in Cwp for these speeds, which would seem very unlikely. However, for low speeds it would appear that Cwp is not varying greatly with yaw. Assuming that the slope of the graph of k_Δ would follow a similar trend at the lower Froude number, ARe can be calculated from the slope of the low Froude number Ct curve. Then if it is assumed that ARe does not vary with speed, the ARe calculated from low speed runs may be used for high speed runs, and then Cdi may be calculated for each run using Equation (9). This procedure has the implication that ARe is dependent on heel angle and vessel parameters only, which mirrors an empirical approach suggested by Gerritsma, 1993, pp 237-238. A physical interpretation of this is that the efficiency of the foil due to three-dimensional effects is only dependent on heel and vessel parameters. Here the reduction of efficiency due to three-dimensional effects is due to tip vortex production, which arises from span-wise flow across the foil.

HULL-APPENDAGE INTERACTION EVIDENT IN WAVE-PATTERN

Overall Effects of Appendages

Upright runs, 0° heel, 0° yaw

Tests were carried out for the basic AMECRC 004 parent hull without appendages, with rudder only, with keel only and with both keel and rudder. By examining the relative resistance components of these runs it is possible to determine the effects each appendage will have on the overall flow around the yacht. The graph of Fig. 4 shows the normalised total resistance components. For each speed the total resistance was normalised by dividing by the maximum total model scale resistance of the four runs for that speed.

The model numbers refer to those given in Fig. 5, error bars have been drawn on this graph based on the random errors from repeatability tests. It can be seen from Fig. 6 that a large increase in resistance is obtained when the keel is added to the model for both cases of with and without a rudder. Fig. 7 is a similar plot of normalised resistance for Rwp, the wave-pattern resistance.

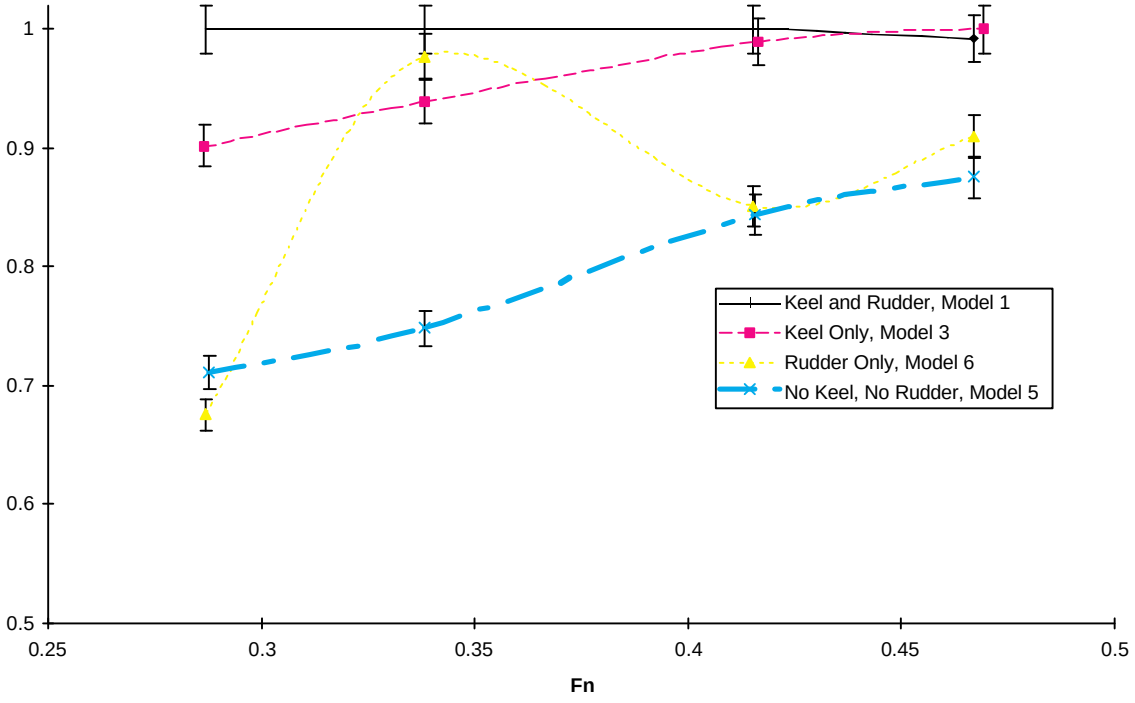

Fig. 8 Effect on Rt of adding appendages (Rt has been normalised)

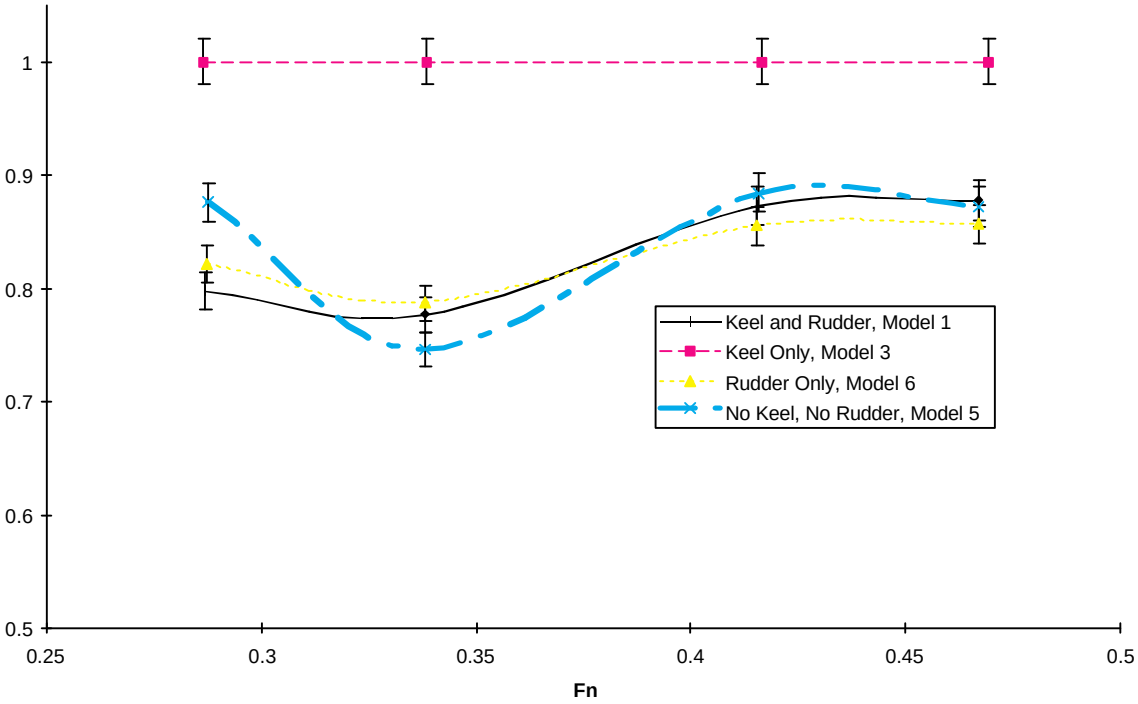

Fig. 9 Effect on Rwp of adding appendages (Rwp has been normalised)

From Fig. 10 it would appear that adding the rudder will nearly always result in a decrease in wave-pattern resistance.

Then taking the total resistance minus the wave-pattern resistance we get the viscous resistance. A plot of the normalised viscous resistance has been shown in Fig. 11. The effect of adding a rudder can be seen to increase the viscous resistance, mirroring the results for the total resistance.

The reduction of wave-pattern resistance by adding the rudder is thought to be due to the wave field created by the rudder, which appears to oppose the wave-pattern of the hull. This was tested theoretically by calculating the positions of the troughs and crests of a Kelvin wave-pattern produced by bodies positioned at the leading edges of the keel and rudder. A detailed description of the graphical method used to calculate crest lines for a Kelvin wave-pattern can be found in Marr, 1994, pp 3-5. The position of the apex of the sectors containing the Kelvin wave-pattern was calculated from a guideline found in Newman, 1977 p 275, in which it is quoted that the apex should be upstream of the bow of a ship typically by one ship length. For the cases of the rudder and the keel one ship length was taken to be the length of the chord at the root of the foil. This pattern was then superimposed on the wave-pattern determined from experiments. It was assumed that if either appendage created a trough where the main hull had a crest it would reduce the overall wave-pattern resistance. The conclusion from this analysis was that adding the keel should increase the wave-pattern resistance, because the crest lines from the keel generally lie on crest lines from the bare hull; whereas adding the rudder should reduce the wave-pattern resistance, because the crest lines lie on troughs from the bare hull. As stated above this is also the conclusion drawn from the wave-cut experiments. The rudder has more effect on the model with keel only (as compared with the bare model) because the waves are larger for this model and so interferences within the wave-pattern have more effect.

However, the addition of the rudder will also add to the viscous drag (both form drag and skin friction). In the runs shown above, except for the highest speed, the increase in Rv due to adding the rudder outweighs the decrease in Rwp. However, at full scale the relative importance of Rv is reduced slightly and so the trends in Rt could be reversed if the scale difference is large enough. For example the normalised total resistance plot of Fig. 12 plotted for full scale is reproduced in Fig. 13.

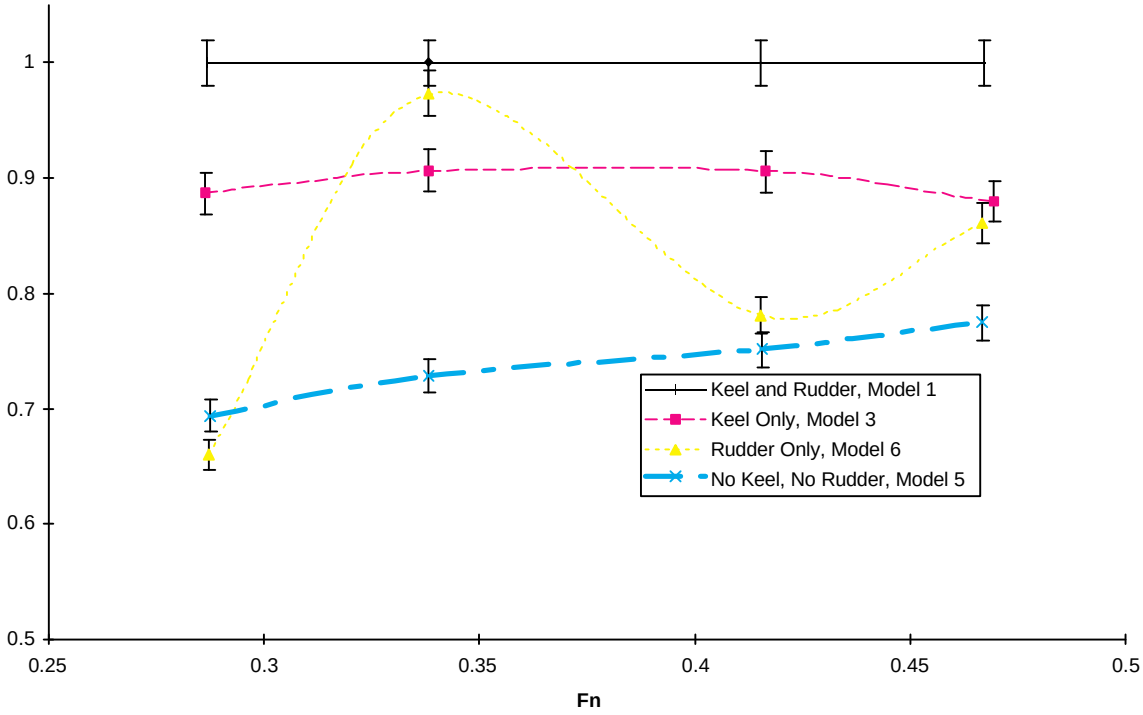

Fig. 14 Effect on Rv of adding appendages (Rv has been normalised)

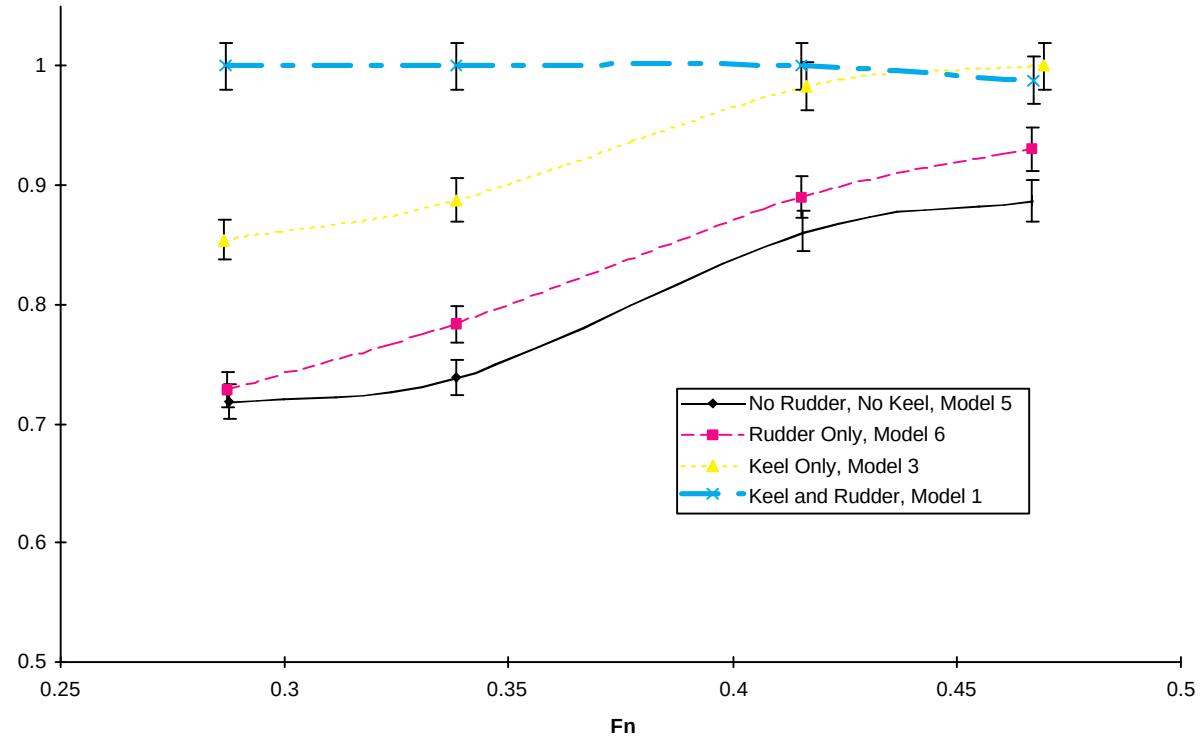

Fig. 15 Full Scale Rt normalised

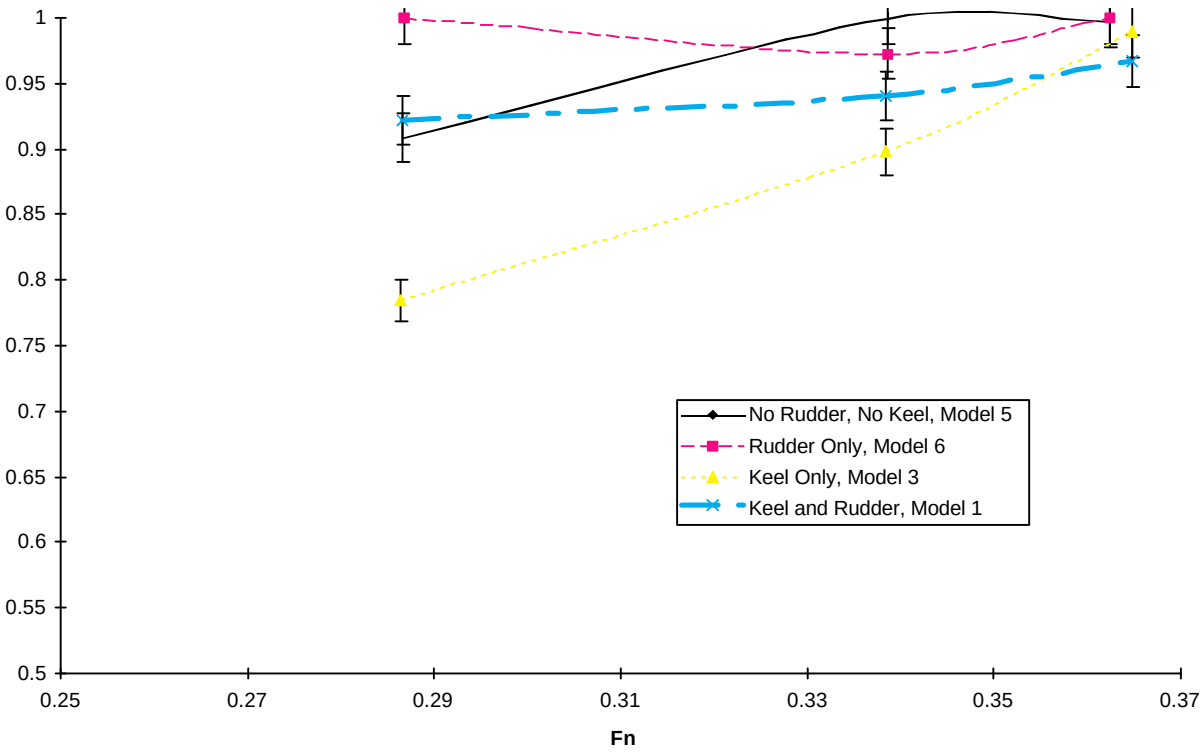

Fig. 16 Rwp normalised for 20° heel 1° yaw

Heeled and yawed runs

The conditions which were examined in detail were for heels of 10° and 20°, and yaws of 1°, 3° and 5°. The same method for normalising the resistance was used, that is dividing by the largest resistance value for each Froude number on the graph. An example of the normalised wave-pattern resistance has been shown in Fig. 17 for 20° heel and 1° yaw. It would appear from the 12 runs presented in Fig. 18, and a further 60 similar runs (not shown here), that the wave-pattern resistance is reduced by adding the keel and increased by adding the rudder under some conditions. Clearly the simple rule of opposing wave fields is not working in these runs. The change in the flow velocity in the midships section due to the lift being produced by the keel has changed the trends in the wave-pattern resistance. However, creating similar flow changes around the stern would appear to produce different trends. Theoretical and experimental investigations have been carried out in other research upon wave-patterns within which lift is being produced. For example wave-pattern research reported by Kuhn and Scragg, 1993, which was conducted on a surface piercing foil. This research found that the wave-pattern resistance would increase with increasing lift on a surface piercing foil. The increase in wave-pattern resistance between the foil at 0° yaw and at 4° yaw was found to be about 60%, which was measured by wave-cut techniques and predicted with inviscid approximations. Therefore the reduction in wave-pattern resistance shown in Fig. 19 with the addition of the keel is thought to be due to interference of the keel wave-pattern and that of the hull.

Also, when the rudder is added to the bare hull the wave-pattern resistance only appears to change at the lowest speed (Fn = 0.286, full scale speed = 5.50 knots), within experimental error. For this speed the bare hull had an average of 13% less wave-pattern resistance for 10° heel 1° yaw, 20° heel 1° yaw and 20° heel 3° yaw. The waves created by the keel in the above conditions would appear to be out of phase with the yacht's wave-pattern thereby reducing the overall resistance. However, if the rudder is added to the hull with the keel attached, the wave-pattern resistance is definitely increased. This would lead to the conclusion that adding the rudder only increases the wave-pattern resistance of the yacht when it is apparently out of phase with the waves created by the keel producing lift, thus adding to the waves created by the hull. The fact that the rudder decreases the wave-pattern resistance for the lowest speed and the small yaw angles for the bare hull would tend to indicate that the same phenomenon is apparent for these runs as is for the upright runs mentioned above. This is quite possible under the hypothesis presented in this paragraph as there is very little lift being produced for this condition.

Fig. 20 is a graph of normalised total resistance for the same heeled and yawed condition.

.

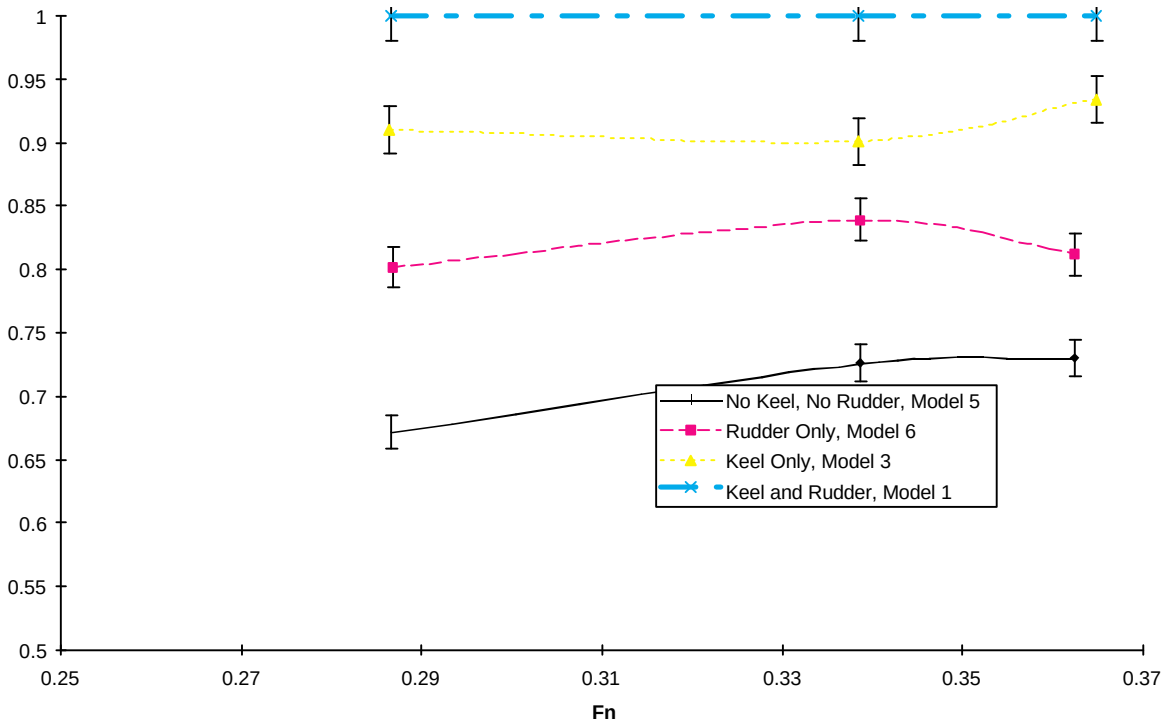

Fig. 21 Rt normalised for 20° heel 1° yaw

Here the total resistance would appear to be following much more predictable trends, in that adding an appendage increases the resistance, and adding the keel increases the resistance more than adding the rudder does. It is also worth noting that the changes in total resistance are much larger than those for the wave-pattern resistance. This would tend to suggest that the effect of adding appendages is mainly seen in the viscous resistance and the induced drag. The viscous resistance has been graphed in Fig. 22.

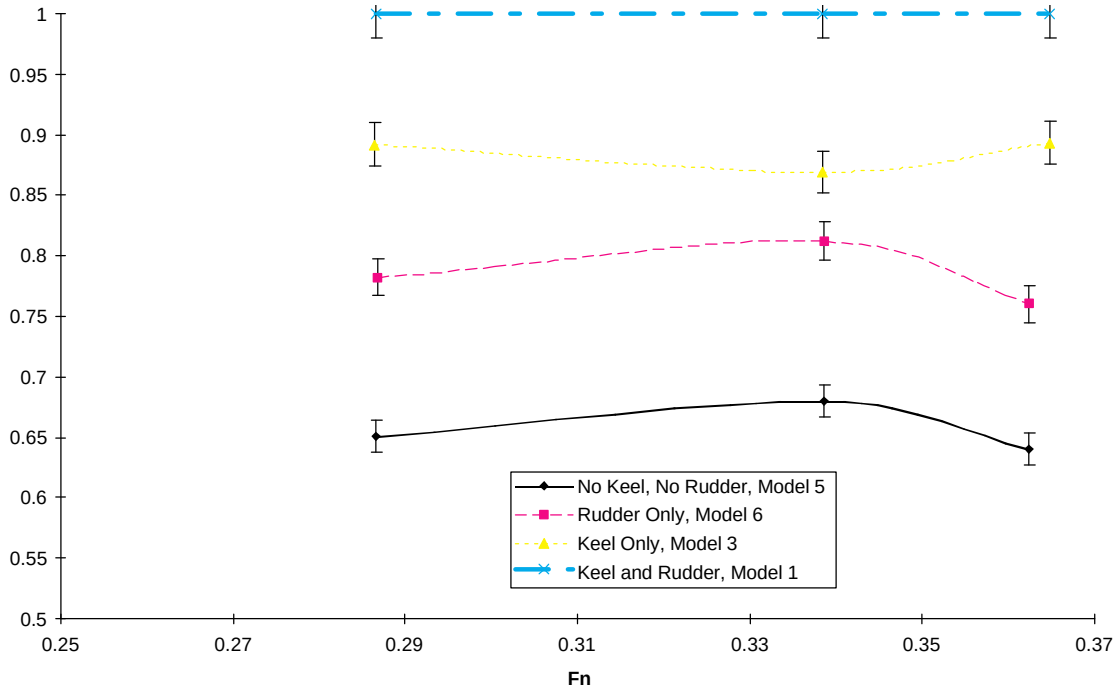

Fig. 23 Rv normalised for 20° heel 1° yaw

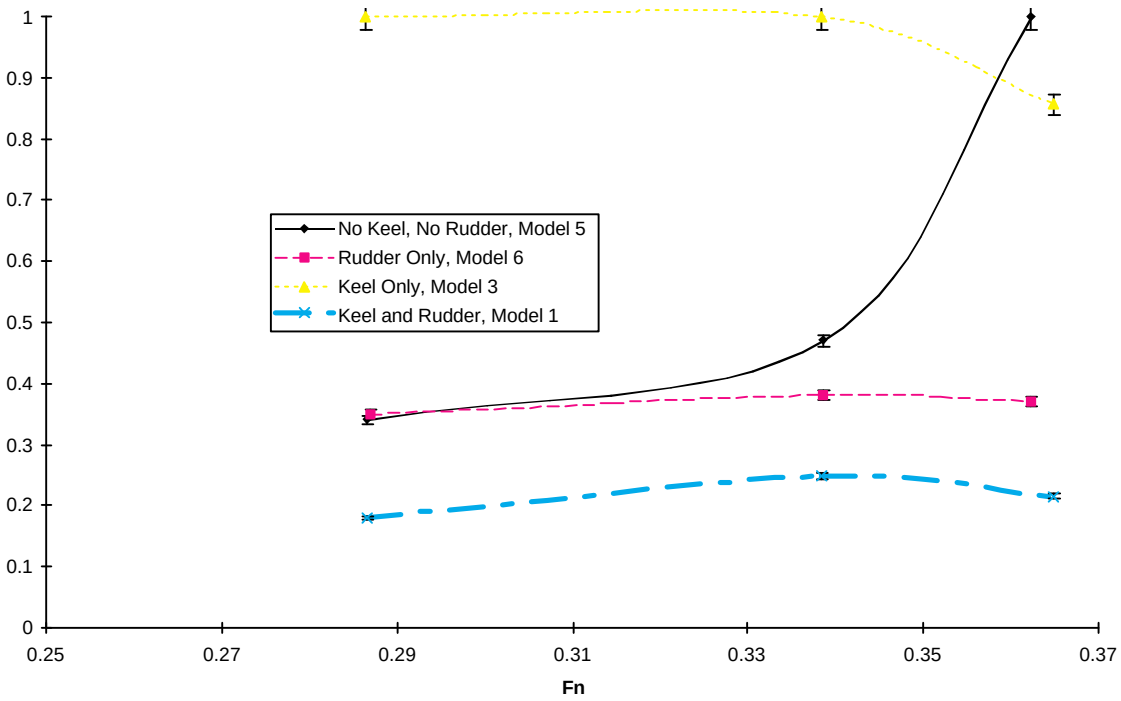

Fig. 24 Calculated Di normalised for 20° heel 1° yaw

Rv of Fig. 25 can be seen to be mirroring that of the total resistance.

Fig. 26 shows the normalised induced drag, calculated using Equation (10). The vertical axis on this graph has been shifted relative to the previous graphs to give a zero origin. The graph appears very strange at first, because the highest induced drag is shown for the model with the keel only. An explanation for this must start with considering that the coefficient of induced drag Cdi is calculated using Equation (11). Therefore, an increase in induced drag is due to either an effective aspect ratio decrease or a lift increase. The calculated effective aspect ratios for the two models show a 30% change, however, the change in induced drag was of the order of 80%. Therefore the lift must have increased for Model 3. This was shown in the experimental results for the lift. For the lowest speed graphed in Fig. 24 the measured model scale lift for Model 3 was 6.78 N, whereas for Model 1 it was 3.36 N.

Model 3 creating more lift than Model 1 appears to show an error, because Model 3 has less lifting surfaces than Model 1. However, the rudder is operating in the downwash of the keel and could therefore produce negative lift. This is also shown by the longitudinal centre of effort of the model, which is further forward for Model 1 than for Model 3. It was calculated (by inviscid theory, see Houghton and Brock, 1970, pp 370-374) that the downwash angle for this model is approximately equal to 70% of the angle of yaw, therefore at one degree yaw and one degree rudder angle relative to the yacht, the rudder is actually at 1.3° to the flow. To make negative lift the rudder is required to be at a negative angle to the flow, therefore either there is an error in the rudder setting or the assumptions required to calculate the downwash angle are not quite valid. The assumptions required are that the keel lift distribution is elliptic, that the rudder is located in the same plane as the wake of the keel (see Houghton and Brock, 1970, pp 371-372) and finally that the flow is not disturbed by the hull of the yacht.

The final assumption has definitely been broken as the bare hull would appear to be capable of turning the flow towards the stern. This can be seen when examining the results for the hull with no keel and no rudder attached. For all of the heeled and yawed runs for this condition, using the sign convention shown in Fig. 27. A positive lift (along the y-axis) was measured with a negative yawing moment about the vertical axis. For most runs with the bare hull it is not possible to calculate with any accuracy the longitudinal centre of effort of the lift force. This is because with the errors on the lift measurement it is essentially zero, but the yaw moment is definitely negative. Therefore, the hydrodynamic forces on the hull create a pure moment on the hull (with no lift). There was, however, one extreme condition run for which it can be calculated that the longitudinal centre of effort is 4.7±2 m forward of the bow. Then by using a method described as slender body theory in Nomoto and Tatano, 1979, pp 76-80, a theoretical prediction for the centre of effort can be calculated. This calculation results in a predicted centre of effort of 3.73 m forward of the bow. Therefore, it can be concluded that the situation seen in the experiments is also predicted to a certain degree in theory.

This is possible if the flow is turned around the yacht, thus providing a negative lift force on the stern of the yacht. The hypothesis can be better understood by examining the following two-dimensional schematic diagram.

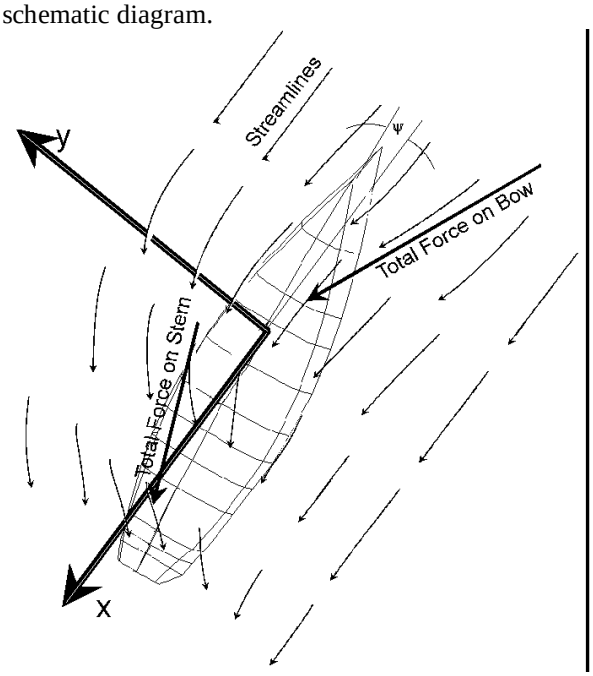

Fig. 28 Possible two-dimensional streamlines to give positive lift and negative yaw moment

Fig. 29 is a view looking up at the bottom of the hull, and shows a possible set of streamlines in one plane which could give a positive lift and a negative yaw moment. This combination will then give a longitudinal centre of effort well forward of the bow, resulting in the yacht wanting to steer to windward, or weather helm. It is therefore possible to give the rudder negative lift, as seen in the results mentioned above.

This feature was further investigated by examining the tests done for 20° heel and 5° yaw. For

this case it was concluded that the rudder was not generating negative lift, as the lift increased and the centre of effort moved aft for Model 1 when compared with Model 3. It is believed that there are two reasons for the difference. Firstly, the rudder would be coming out of the plane of the wake of the keel, thus reducing the velocity of the fluid from the tip and root vorticies of the keel, therefore reducing the downwash angle. Secondly the yacht is turning the flow at the stern less at higher angles of yaw.

However, the use of a single post dynamometer makes the investigation of rudder lift difficult. This is because the yaw angle and the rudder angle are not known with high accuracy . Also the post can twist slightly due to the yaw moment experienced by the model. It is believed at this stage that the single post dynamometer has not introduced errors which affect the conclusions above. For these reasons the phenomenon described as negative lift on the rudder is the subject of further investigation.

Keel Rudder Separation Effects

Upright runs

Tests were carried out on three different models with varying keel rudder separation. Model 1 had the rudder in the design position, Model 2 had the rudder moved aft, and Model 4 had the rudder moved forward. The same analysis used above was carried out, resulting in the graph shown as Fig. 30 for the normalised wave-pattern resistance. The lowest speed seems to show very little change in wave-pattern resistance. The middle speed in the above graph shows the largest change in Rwp for the conditions considered. At this speed the rudder forward appears to have the lowest value for Rwp, which is thought to be due to smoothing the section area curve. Smoothing the section area curve is known to reduce the wave-pattern resistance, for example see Keuning and Kapsenberg, 1995, p 138. The same plot for total resistance is shown in Fig. 31.

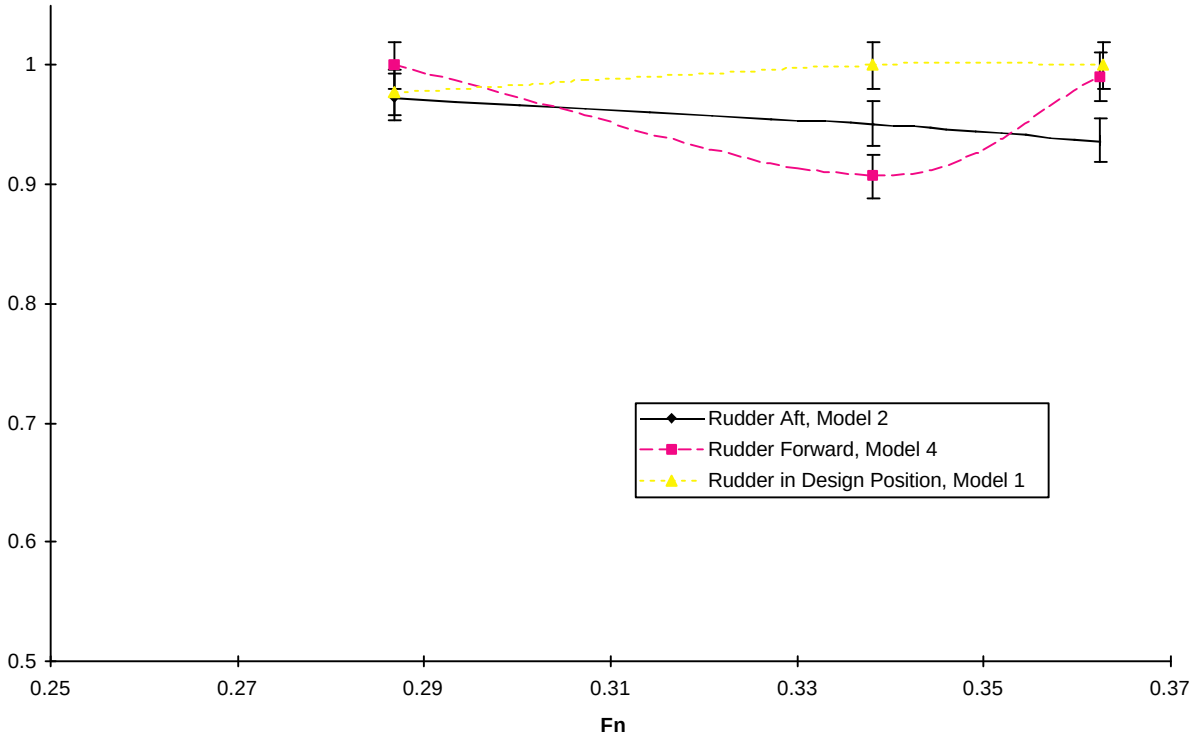

Fig. 32 Effect on Rwp of keel rudder separation (Rwp has been normalised)

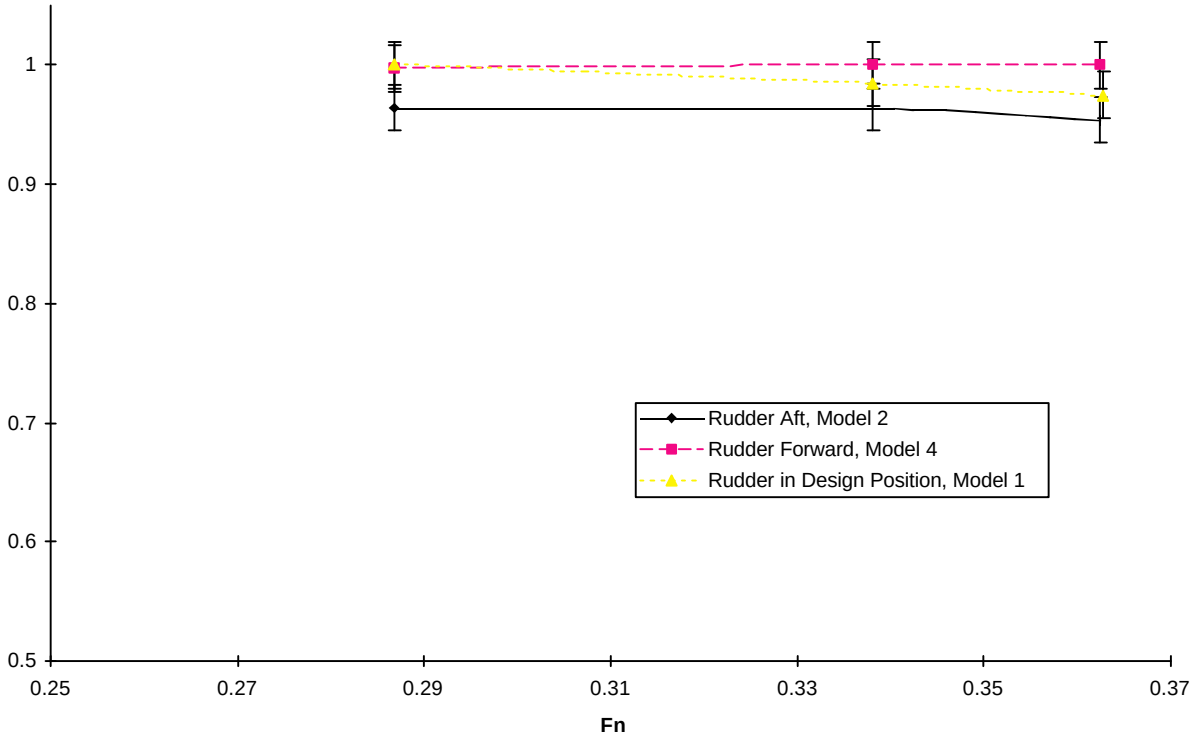

Fig. 33 Effect on Rt of keel rudder separation (Rt has been normalised)

The values plotted in Fig. 34 are extremely close together, therefore it can be assumed that at model scale the total resistance is not affected very much by keel rudder separation. A definite trend is evident suggesting that the further the rudder is moved aft the lower the total resistance will be. Fig. 35 is a plot of the viscous resistance normalised with respect to the maximum value of the three models as above

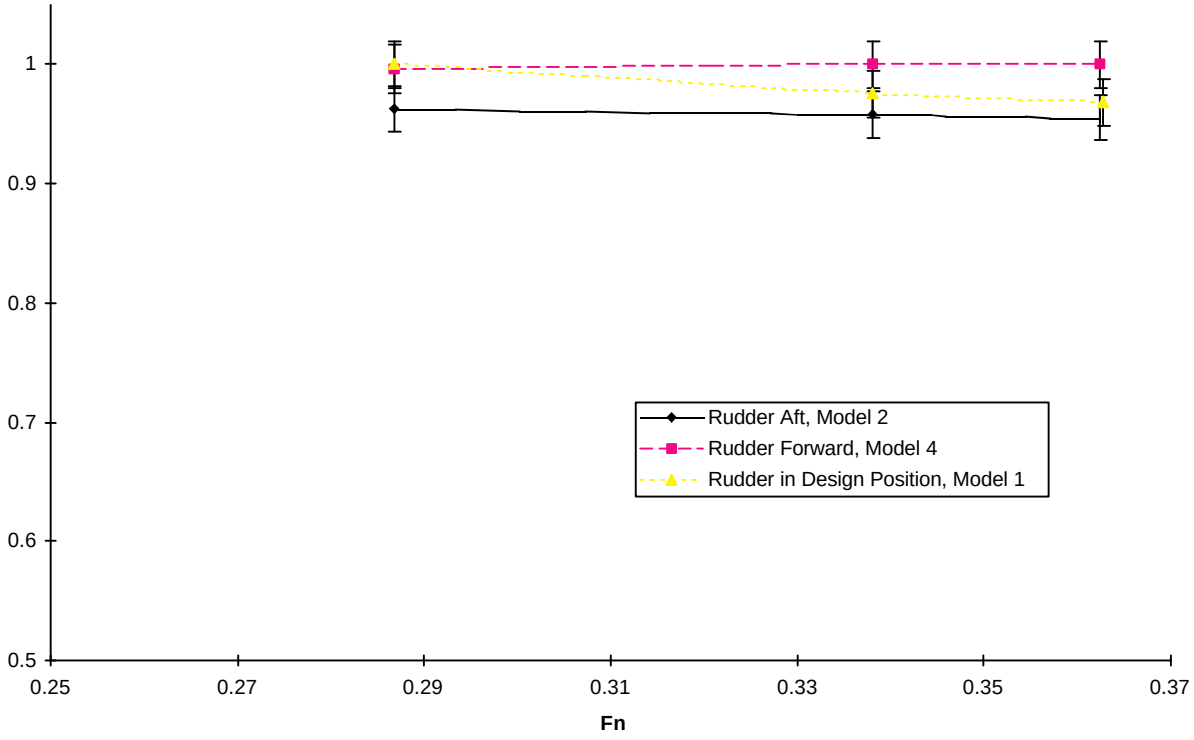

Fig. 36 Effect on Rv of keel rudder separation (Rv has been normalised)

Again this graph mirrors that of the total resistance, as most of the resistance is viscous resistance for these runs. Typically the viscous resistance makes up between 80-90% of the total resistance for these runs. As mentioned previously the rudder tends to emerge at higher speeds, due to large trimming moments being applied, which could account for a lot of the reduction in viscous resistance. This goes against the general rule of thumb which says that the larger the buttock angle the larger will be the viscous resistance. By the above observations it would appear that the rudder emerging outweighs this usual effect.

The largest changes are evident in the wave-pattern resistance thus indicating that the wave-pattern resistance is more sensitive to changing the keel rudder separation.

Remaining Conditions

The remaining conditions to be considered are all heeled and yawed runs for which the keel rudder separation was varied and the rudder angle was varied. To draw definite conclusions for these runs is very difficult as so many variables are changing which need to be considered. It is for these reasons that the analyses presented above shall not be presented for these series. To get a better appreciation of what is actually happening a more detailed picture of the flow around the yacht is required.

Nevertheless the wave-pattern resistance shows a much greater difference than the total resistance when these conditions are changed. The viscous resistance constitutes the larger portion of the total resistance, and so it follows the trends of the total resistance. For example considering a low speed run, a change of 12% is evident in the wave-pattern resistance, whereas a change of only 2% is evident for the total resistance.

In the analysis presented above the interaction effects on the lift of the yacht have not been discussed. However, the change in lift due to the variables examined has been included in the following VPP analysis.

DESIGN GUIDELINES FROM CURRENT WORK

The purpose of the research explained in this paper, as stated previously, is to provide design information as to the effects of hull-appendage interaction on resistance and performance. To accomplish this aim the final product must be an assessment of the relative performance effects of this interaction. The changes introduced as a result of this research have two main features. Firstly the resistance is scaled differently, and then the effects of the rudder variables are incorporated into the VPP.

Scaling Modification Effects

The changes in scaling when the wave-cut results are used have been explained above. It is sufficient here to realise that when using a traditional method of scaling, the wave-pattern resistance (here equated to the wave resistance) has been severely overestimated as compared with a wave-cut guided scaling method. Since the viscous resistance for a full scale prototype is less than the viscous resistance for a model, the total full scale resistance is reduced. Therefore the predicted velocity of the yacht will be increased. The average increase in yacht velocity was calculated to be 1.44%. From experience it is known that using tank results to predict full scale speed generally under-predicts the performance of the full scale yacht, the change to scaling methods presented here could therefore go to explain some of the difference.

To get an overall picture of the yacht's performance the General Purpose Rating (GPR) can be considered. This is a measure of a yacht's performance calculated from the VPP results. The units of the GPR are seconds per nautical mile. The wind conditions are an average of results for 8 knots and 12 knots of true wind for a linear random (LR) course. The LR course is a standard course used in the IMS handicapping system, it consists of considering that the yacht sails a straight course and that the wind angle varies for equal amounts of time between 0° and 180°. The calculated GPR figure shows a change of -2.5% when the wave-cut scaling procedure is used.

Errors in performance indicators

For the analysis presented here the most important errors are the random errors in the data. Systematic errors are of course important when considering the actual performance prediction, however these cannot be fully described without more validation, such as full scale tests.

A series of repeat runs was used to identify the random errors in the wave-pattern record. This gave an error of ±0.2 mm in the measured wave heights. Then the systematic errors were estimated for the wave-cut spacing measurement. These two errors were added to wave-pattern profiles as Gaussian random noise and the data was reanalysed, the difference between the results for the original data and the artificially corrupted data was taken to be the error. This procedure was repeated five times for each run investigated, with different random noise. It was

calculated that the known errors present in the wave-pattern resistance due to incorrect readings were 1.5%. The regression process used to incorporate the results into the VPP, by virtue of the averaging nature of regression, should help to reduce some of this error. Therefore it can be said that the total random error in resistance predictions should be less than 1.5%.

If it is assumed that a percentage change in the resistance is linearly proportional to the resulting percentage change in performance indicator, then the maximum percentage errors in each performance indicator can be calculated. Using the cases presented above, an average change in total resistance of -11.6% resulted in an average velocity change of 1.4% and a GPR change of -2.5%. Therefore if an error of 1.5% was present in the total resistance value, this would correspond to an error of 0.2% in the velocity prediction and 0.3% in GPR.

Rudder Variables Effects on Yacht Performance

The effects on the yacht's performance due to the rudder variables investigated were found to be very small. Typically the changes in velocity were of the order of less than 1%. Therefore it was considered the changes in velocity were too small to draw any meaningful conclusions from polar plots of the yacht velocity. Instead the calculated GPR (defined above) can be compared for each rudder variation.

It is important to run a base case for the yacht performance first, which gives the change in predicted performance due to the wave-cut scaling technique. This was done for the full scale yacht with a keel rudder separation of 4.75 m (measured from the leading edge of the keel to the leading edge of the rudder, positive in the aft direction) and a rudder angle equal to the yaw angle at all times. This condition corresponds to the design test condition.

The way in which GPR changes with the two variables investigated is plotted in Fig. 37. In Fig. 38 the rudder angle is relative to the centre line of the yacht. From this figure it can be concluded that moving the rudder aft from the design position will marginally improve the performance of the yacht, by just greater than the random error. Moving the rudder forward by the same amount has exactly the opposite effect. Keeping the rudder at an angle of 0° appears to improve the yacht's performance by a marginal amount, whilst setting it to 5° appears to do the opposite. The greatest improvement is obtained by moving the rudder aft and reducing the rudder angle to 0°, whereas the worst performance is obtained by moving the rudder forward and setting the angle to 5°.

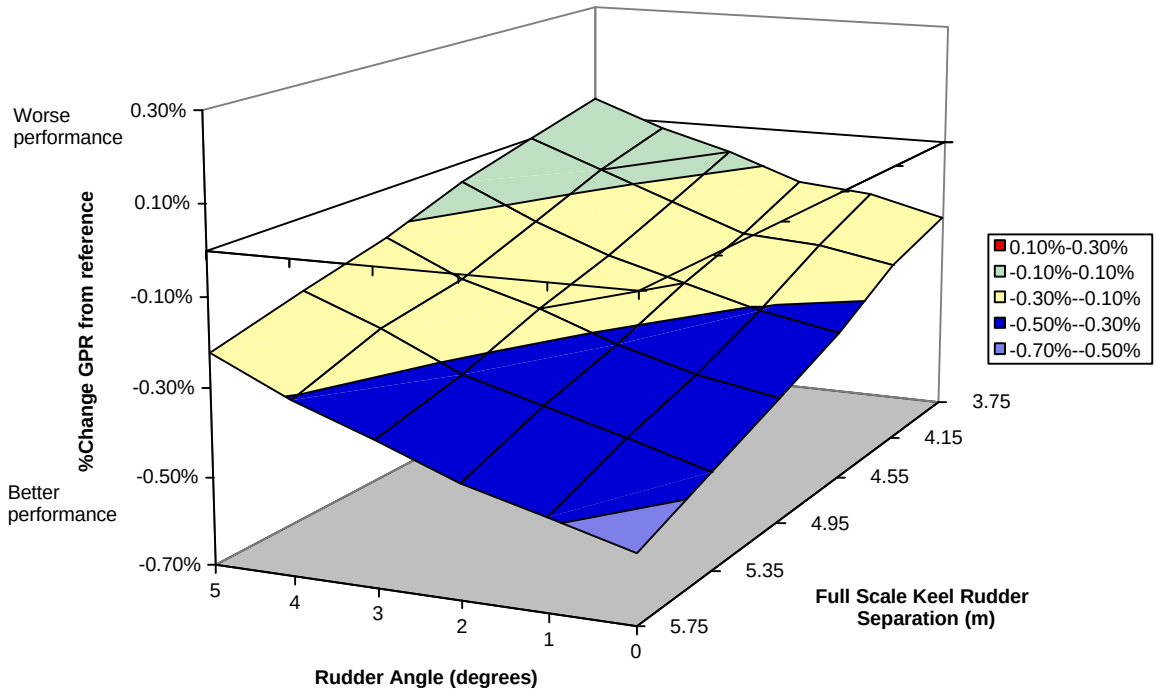

Fig. 39 Surface plot of % variation in GPR with rudder angle and keel rudder separation

CONCLUSIONS

Firstly for the test conditions which involved simply adding the appendages the total resistance follows fairly expected trends. For example adding the keel tends to increase the total resistance more than adding the rudder does. However, these trends are not evident in the wave-pattern resistance, because of the interference effects on the flow around the yacht. The expected trends are therefore due mainly to viscous and induced drag differences resulting simply from the increase in wetted area and associated form drag. The hull-appendage interference drag can therefore be better understood by wave-cut type analysis. Another approach has been taken in the past where an empirical formula is used to estimate the viscous interaction forces, see for example Teeters, 1993.

Trends within the runs which involved changing appendage parameters were much more difficult to find. However, the changes were much more evident in Rwp than Rt or Rv, therefore appendage variations do actually show themselves more in the wave-pattern than in the total resistance which is dominated by viscous effects. The exact nature of the interference effects is difficult to decipher without a greater knowledge of the flow patterns around the yacht.

The stated aim of this project was to provide design information as to the effects of hull-appendage interaction on the performance of a sailing yacht. The assumption that the interaction forces would be most evident in the wave-pattern resistance was examined by conducting wave-cut experiments that are constructed to measure the resistance associated with creating the inviscid wave-pattern produced by a model yacht. By showing that variables which should affect the interaction forces the most also result in a large change in wave-pattern resistance relative to the total resistance, it has been reasoned that this assumption was correct.

Regardless of the reasoning, the question still remains as to whether or not design information has been provided. The answer to this question lies in the work presented concerning the performance indicators, in which it is concluded that varying the rudder angle and the keel rudder separation suggests that the rudder should be put as far aft as possible and the rudder angle should be set as low as possible.

ACKNOWLEDGMENTS

This paper is based on research conducted as a part of the Australian Maritime Engineering CRC's Yacht Technology and Performance research program.

The authors would like to thank the following for their help during experiments and data analysis Giles Thomas, Bruce McRae, Roy Horne, Martin Shaw, Mark Lees, Damien Freeman, Ben Church and Warwick Oliver.

REFERENCES

Binns, J. "Hull-Appendage Interaction of a Heeled and Yawed Vessel", to be submitted for MSc Thesis, Curtin University of Technology, 1996

Duncan, W.J., Thom, A.S., and Young, A.D., *Mechanics of Fluids,* Edward Arnold, London, 1970

Eggers, K.W., Sharma, S.D., Ward, L.W., "An Assessment of Some Experimental Methods for Determining the Wavemaking Characteristics of a Ship Form", *Trans SNAME*, 75, 1967, pp 112-157

Gerritsma, J., Keuning, J.A. and Versluis, A., "Sailing Yacht Performance in Calm Water and Waves", *The 11th Chesapeake Sailing Yacht Symposium*, 1993, pp 233-245

Harvald, S.A., *Resistance and Propulsion of Ships,* Wiley-Interscience, New York, 1983

Hogben, N. and Standing, R.G., "Wave Resistance from Routine Model Tests", *Trans. RINA*, 1974, pp 279-295

Houghton, E.L. and Brock, A.E., *Aerodynamics for Engineering Students,* Edward Arnold, London, 1970

Hughes, G., "An Analysis of Ship Model Resistance into Viscous and Wave Components Parts I and II", *Trans. RINA*, 108, 1966, pp 289-302

Keuning, J.A. and Kapsenberg, G.K., "Wing-Body Interactions on a Sailing Yacht", *The 12th Chesapeake Sailing Yacht Symposium*, 1995, pp 133-144

Kuhn, J.C. and Scragg, C.A, "Analysis of Lift and Drag on a Surface-Piercing Foil", *The 11th Chesapeake Sailing Yacht Symposium*, 1993, pp 277-288

Marr, G., "An Introduction to the Computation of Wave Resistance for Yacht Design", *The International Yacht Design Symposium*, 1994

Newman, J.N., *Marine Hydrodynamics*, MIT Press, London, 1977

Nomoto, K. and Tatano, H., "Balance of Helm of Sailing Yachts", *HISWA Sailing Yacht Symposium*, 1979, pp 65-89

Rosen, B.S., Laiosa, J.P., Davis, W.H. and Stavetski, D., "SPLASH Free-Surface Flow Code Methodology for Hydrodynamic Design and Analysis of IACC Yachts", *The 11th Chesapeake Sailing Yacht Symposium*, 1993, pp 35-49

Teeters, J.R., "Refinements in the Techniques of Tank Testing", *11th Chesapeake Sailing Yacht Symposium*, 1993, pp 13-34

APPENDIX A: SUMMARY OF WAVE-CUT PROCEDURES

The methods by which the figures presented in this paper have been calculated are detailed in Binns, 1996. The following is a brief description of how the wave-cut results can be obtained, without any proofs or error estimates.

Probe Spacing

Longitudinal cuts were performed using 8 channels of capacitance wave probes across the test-tank. The position of the probes from the start of the run was 45 m and the spacing between the probes was set as close to the tank width divided by ten as possible. The cut spacing was suggested by Hogben and Standing, 1974, p 295, however it was felt that it would be better to try and place at least one cut at the position of the tank width on four. This conclusion was reached by examining which wave-number component of the total resistance was always very large, and then calculating which position should measure the greatest change in this wave-number component. To check this hypothesis more tests would have to be conducted, with a probe positioned at this spacing.

It is worth noting here that the probe spacing should be measured as accurately as possible. Serious systematic errors can be introduced if this is not done. An acceptable accuracy for this measurement would be ±1 mm.

Data acquisition

It is considered that the signals were adequately filtered, through use of carefully designed analog and digital filters. The number of samples to be taken for each run can be calculated from the following equation

$$N = A\frac{LWL}{Vs} \times R + B, \qquad (12)$$

where LWL is the waterline length of the model in metres, Vs is the model speed in m/s, R is the sample rate in Hz and A and B are coefficients. The coefficient A is the number of boat lengths to use (here taken as 6), and B is the number of samples which are redundant (here taken as 600).

Multiple Longitudinal Cut Method Used

The method used to calculate the wave-pattern resistance is best described as a least squares multiple longitudinal cut method. A summary of the procedure follows.

Symmetric Analysis

Through consideration of the wave potential of a Kelvin wave-pattern it can be shown that the wave heights can be described by the following equation

$$\zeta(x,y) = \frac{1}{2}\sum_{n=-\infty}^{n=\infty}\begin{pmatrix} A_n \cos(\alpha_n x) \\ +B_n \sin(\alpha_n x)\end{pmatrix}\cos(\beta_n y), \qquad (13)$$

where,

$$\alpha_n = \gamma_n \cos\theta_n,$$
$$\beta_n = \frac{2n\pi}{b}, \qquad (14)$$
$$\gamma_n \cos^2\theta_n = K\tanh\gamma_n h,$$
$$K = \frac{g}{Vs^2},$$

and

$$K\sin\theta_n \sec^2\theta_n = \frac{2n\pi}{b}.$$

In the above expressions θ_n is the propagation angle of the nth wave component, b is the tank width, Vs is the vessel velocity and g is the acceleration due to gravity. Then a least squares solution to Equation (15) can be calculated from model wave heights obtained. The total wave-pattern resistance can be calculated from

$$Rwp = \frac{\rho g b}{8}\left[\begin{array}{l} 2\left(2-\frac{Q_0K^2}{\alpha_0^2}\right)\left(A_0^2+B_0^2\right) \\ +\sum_{n=1}^{\infty}\left(2-\frac{Q_nK^2}{\alpha_n^2}\right)\left(A_n^2+B_n^2\right)\end{array}\right], \qquad (16)$$

where,

$$Q_n = \tanh^2 \gamma_n h \left[1 + \frac{2\gamma_n h}{\sinh 2\gamma_n h} \right].$$

Asymmetric Analysis

It can be shown that an asymmetric wave-pattern can be described by the following equation

$$\zeta(x,y) = \frac{1}{2} \sum_{n=-\infty}^{n=\infty} \begin{pmatrix} A_n \cos(\alpha_n x) \\ +B_n \sin(\alpha_n x) \end{pmatrix} \cos\left(\beta_n \left(y - \frac{b}{2} \right) \right) \qquad (17)$$

then the same equations can be used as for the symmetric analysis with the exception of Equation (18), which becomes

$$\beta_n = \frac{n\pi}{b}. \qquad (19)$$

It can be seen that odd values of n in Equation (20) describe asymmetric waves and even values describe symmetric waves. The asymmetric analysis can therefore also be used for symmetric patterns, however this is inadvisable as extremely ill-conditioned matrices result from the least squares analysis.